BIOCHEMISTRY
including biophysical chemistry & molecular biology

Article

pubs.acs.org/biochemistry

Mutants of Metal Binding Site M1 in APP E2 Show Metal Specific Differences in Binding of Heparin but Not of sorLA

Christian Dienemann,[†,§] Ina Coburger,[†] Arnela Mehmedbasic,[‡] Olav M. Andersen,[‡] and Manuel E. Than*[,†]

[†]Leibniz Institute for Age Research, Fritz Lipmann Institute (FLI), Protein Crystallography Group, Beutenbergstrasse 11, 07745 Jena, Germany

[‡]The Lundbeck Foundation Research Center MIND, Danish Research Institute of Translational Neuroscience (DANDRITE) Nordic-EMBL Partnership, Department of Biomedicine, Aarhus University, Ole Worms Allé 3, DK-8000 Aarhus C, Denmark

Supporting Information

ABSTRACT: The amyloid precursor protein (APP) and its neurotoxic cleavage product Aβ are key players in the development of Alzheimer's disease (AD) and appear to be essential for neuronal development and cell homeostasis. Proteolytic processing of APP and its physiological function depend on its interaction with heparin and are influenced by the binding of metal ions and sorLA. We created various mutations of metal binding site M1 residing within the extracellular E2 domain of APP. Using isothermal titration calorimetry and circular dichroism spectroscopy, we analyzed the binding of Cu^{2+} and Zn^{2+} to APP E2 and identified two mutations that are most suited for functional studies to dissect ion specific effects of metal binding. The H313A mutation abrogates only copper-based effects, whereas the H382A mutation weakens any metal binding at M1 of APP E2. Subsequently, we tested the effect of Cu^{2+} and Zn^{2+} on the binding of heparin and sorLA to APP E2 using a chromatographic technique and surface plasmon resonance. We show that Zn^{2+} and to a larger degree also Cu^{2+} enhance the binding of heparin to APP E2, consistent with an extracellular regulation of the function of APP by both metal ions. In contrast, neither ion seemed to affect the interaction between APP E2 and sorLA. This supports an intracellular interaction between the latter two partners that would not sense extracellular variations of metal ions upon synaptic activity.

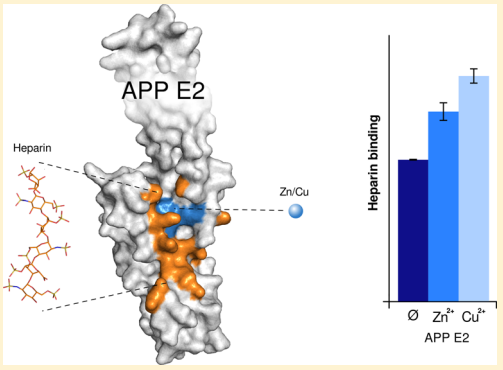

One of the most frequently occurring age-related diseases is dementia with nearly 60−80% of its cases diagnosed as Alzheimer's disease (AD).[1] This accounts at present for more than 5 million patients alone in the United States and makes in this country AD a leading cause of death, with currently one in three seniors dying with AD.[2] A diagnostic hallmark of AD is the development of senile plaques in the brains of respective patients. Those plaques mainly consist of the neurotoxic amyloid β peptide (Aβ), which is proteolytically derived from the amyloid precursor protein (APP) by sequential β- and γ-secretase cleavages.[3] A central hypothesis for the development of senile plaques is an imbalance of Aβ production versus clearance,[4] and the pathological increase in the effective Aβ level has been observed in many studies.[5] In contrast to this strong tie to the etiology of AD, the physiologic function of APP is currently largely unclear. Also, it is matter of an ongoing debate, yet quite conceivable, that the neurotoxicity of Aβ is the primary cause of AD (reviewed in ref 6). In either case, APP, its processing, and potentially also its physiologic (dys)function are tightly linked to the development of AD.[7] Various studies of APP and its interaction with various partners strongly suggest a function in neuronal development and/or homeostasis such as a function in synaptic outgrowth,[8] metal binding and transport,[9,10] regulation of gene transcription,[11,12] cell−cell interaction,[13,14] and/or receptor function.[15]

The amyloid precursor protein underlies a rapid turnover. It is initially sorted to the ER and Golgi and then transported to the cell surface.[16] There, α-secretase cleaves APP and releases the soluble fragment sAPPα. Various studies assigned positive effects on cell growth, cognitive function, and synaptic density to this extracellular fragment (reviewed, e.g., in ref 3). Uncleaved APP becomes reinternalized into endosomal compartments where β- and γ-secretase cleave and thereby produce Aβ.[17−19] APP remains for only a rather short time at the cell surface before it becomes reinternalized. It is yet unclear what regulates the cellular transport and surface exposition of APP and hence the production of the neurotoxic Aβ. A candidate for modulating APP processing is the cell-sorting receptor sorLA that interacts with APP.[20] Also, copper was shown to alter APP trafficking in neurons by down-regulating APP endocytosis,[21] and Zn^{2+} was recently shown to affect, e.g., the oligmerization behavior of the APP orthologue

Received: February 4, 2015
Revised: March 31, 2015
Published: April 2, 2015

DOI: 10.1021/acs.biochem.5b00111
Biochemistry 2015, 54, 2490−2499

APLP1.[22] In addition, the concentration of both metal ions has been shown to be largely altered in the brain interstitium during synaptic activity (reviewed in ref 23). Dysregulated homeostasis of metal ions in the brain has also been implicated in many studies to be correlated with the occurrence of AD, making metal chelators potential drugs for anti-AD treatment.[24]

Human APP is expressed in different splice variants and has two homologues, APLP1 and APLP2, together belonging to the APP protein family.[25] APP is a type 1 transmembrane protein consisting of extracellular domains E1 and E2 that are connected to one another by the flexible acidic region (AcD) and to its single transmembrane helix by the likewise flexible juxtamembrane region (JMR).[26,27] The cleavage sites of the secretase enzymes resides C-terminal of the E2 domain. Larger APP splice variants also possess the Kunitz protease inhibitor (KPI) domain between AcD and E2. Further, APP contains the small intracellular domain (AICD) that has been implicated in signaling.[28]

The E2 domain of APP [also the central APP domain (CAPPD)] is the most conserved domain of APP. It harbors the competitive copper and zinc binding site M1 of high affinity.[10] Histidines 313, 382, 432, and 436 (numbering of APP_{695}) coordinate Cu^{2+} ions with nanomolar affinity (Figure 1A). Zn^{2+} ions are coordinated with micromolar affinity in a

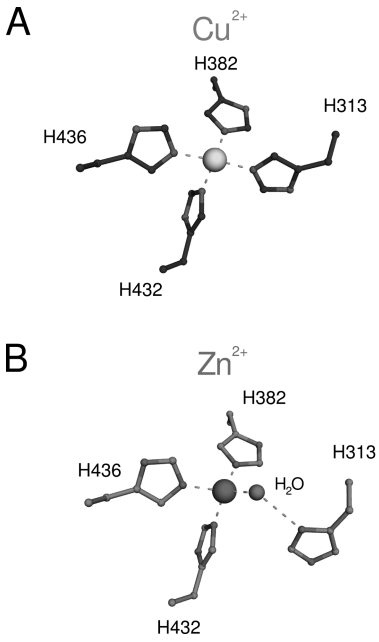

Figure 1. Coordination of (A) copper and (B) zinc at the M1 site of APP E2 according to the coordinates of ref 10.

tridentate manner, involving only three (H382, H432, and H436) of the four Cu^{2+} ligands that are complemented by a water molecule as the fourth ligand (Figure 1B). Binding of these metal ions changes the overall conformation of the E2 domain in a metal ion-dependent manner, which is evidenced by crystal structures and biochemical assays. Histidine 313 of helix α-B is hereby unique in that it contributes to only copper binding but not to zinc binding. Therefore, binding of copper and zinc to M1 has been proposed to represent a central regulatory event for the interaction of APP with specific binding partners.[10] Such interaction partners include heparan sulfates (HS),[29] the neuron growth-regulating F-Spondin,[15] and the cell-sorting receptor sorLA.[20,30]

The binding of HS to the E2 domain also contributes to APP's function as a cell adhesion protein[31] and plays an important role in neurite outgrowth and synapse formation (reviewed, e.g., in ref 32). The affinity of APP E2 for heparin was reported to be regulated by zinc binding.[29] sorLA is genetically associated with the onset of AD, first described as a susceptibility gene for late onset AD (LOAD)[33] and lately confirmed by several genome-wide association studies (GWAS).[34,35] The prevalent model of sorLA function in relation to AD is as a sorting receptor for APP, in particular working as an intracellular gatekeeper that determines the exit of APP from the Golgi whereby sorLA activity decreases Aβ production.[20,36,37] Additionally, sorLA in concert with the retromer complex is also reported to assist in the escape of APP from amyloidogenic processing in the endosomal system.[38−40]

We describe here the generation of various M1 mutants and their biochemical characterization with respect to the binding of copper and zinc ions. Subsequently, we used them to investigate the impact of binding of the metal to the E2 domain on heparin affinity and on the interaction of APP E2 with sorLA to study the complex interplay between metal ions and AD.

MATERIALS AND METHODS

Generation, Expression, and Purification of APP E2 and Its Mutants. M1 site mutants were generated by polymerase chain reaction-based site-directed mutagenesis of pCK3 plasmid DNA[41] encoding human APP_{695} residues 295−500 basically following the QuikChange site-directed mutagenesis approach. The following self-complementary primers were used for mutagenesis: 5′-GTATCTCGAGACACCTGGCGATGAGAATGAAGCGGCCCATTTCCAGAAAGCCAAAG-3′ (H313A), 5′-CGAGAGACAGCAGCTGGTGGAGACAGCGATGGCCAGAGTGGAAGCCATGCTCAATG-3′ (H382A), 5′-GAACAGAAGGACAGACAGGCGACCCTAAAGCATTTCGAACATGTGCGCATGG-3′ (H432A), 5′-CAGAAGGACAGACAGCACACCCTAAAGGCGTTCGAACATGTGCGCATGGTGGATC-3′ (H436A), and 5′-GAACAGAAGGACAGACAGGCGACCCTAAAGGCGTTCGAGCATGTGCGCATGG-3′ (H432+436A).

The thermal cycling protocol included initial denaturation for 60 s, 30 cycles of 95 °C denaturation for 30 s each, 60 s at 55 °C for primer annealing, and elongation for 6 min at 72 °C with PfuPlus! polymerase (Roboklon). Wild-type and mutant APP E2 were expressed in *Escherichia coli* BL21(DE3)RIL and purified without a His tag according to the protocol described for WT APP E2.[10] In short, purification was performed by Ni affinity, heparin affinity, and size exclusion chromatography. The His tag was removed after the Ni step with 0.15 μg of V8 protease/mg of protein for 16 h at 20 °C. All preparations were tested in limited proteolysis experiments (as described in ref 10) to assess the absence of metal ions in the M1 site (not shown).

Isothermal Titration Calorimetry. Isothermal titration calorimetry (ITC) was used to quantify the binding of zinc and copper to mutant APP E2; 400 μM metal and 40 μM protein solutions were prepared in 20 mM Hepes (pH 7.3) and 50 mM Tris (pH 7.3) including 150 mM NaCl for Zn^{2+} and Cu^{2+} measurements, respectively, and degassed before being used. Titration experiments were conducted in a Nano ITC isothermal titration calorimeter (TA Instruments) by 41 injections of 6 μL of a metal solution into protein every 480 s while the samples were being stirred at 250 rpm. All

DOI: 10.1021/acs.biochem.5b00111
Biochemistry 2015, 54, 2490−2499

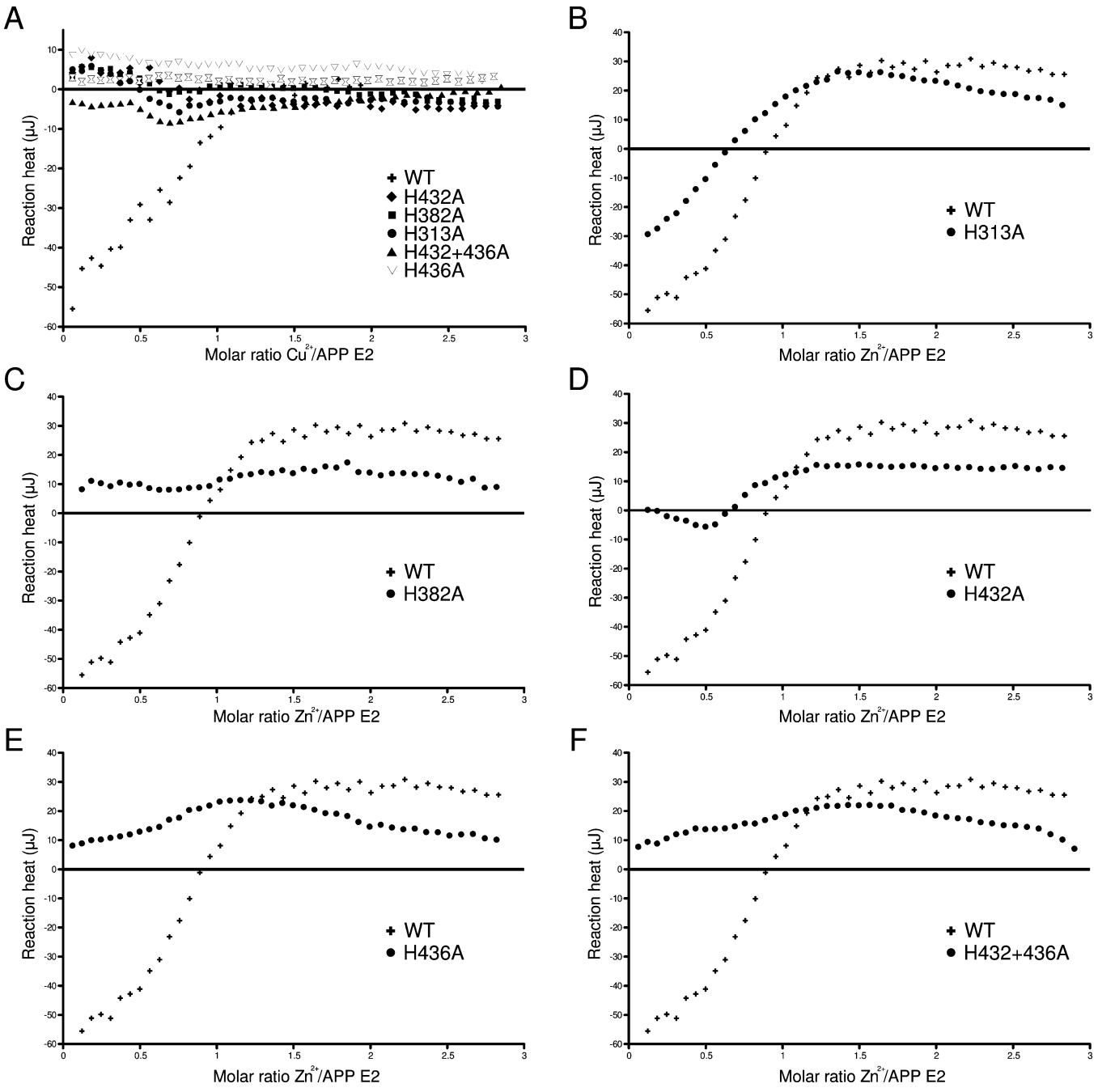

Figure 2. Integrated reaction heats for mutant APP E2 measured with (A) copper and (B–F) zinc. Data of WT APP E2 are shown as black crosses for comparison.

measurements were performed at 20 °C. Blank titrations of metal solutions in buffer were subtracted from recorded peak integrals, and data were analyzed with a NanoAnalyzer (TA Instruments). Data for copper binding experiments were fit to a model assuming a single binding site, whereas zinc binding data were fit with a model for multiple binding sites. As no statistically significant fit of the observed heat to the weaker binding sites of Zn^{2+} to either WT or mutant APP E2 protein was possible as already observed previously,[10] only the thermodynamic data for binding to the tight Zn^{2+} site are considered here.

CD Spectroscopy. CD melting curves at 222 nm were recorded for 7.5 μM WT or mutant APP E2 in ITC buffer supplemented with 10 μM $ZnCl_2$ or $CuCl_2$ by increasing the temperature from 20 to 90 °C in 1 °C steps with a slope of 1 °C/min. Complete CD spectra at 20 °C were recorded before each experiment. Control experiments were conducted without addition of metal solutions. To correct for general differences in the CD signal between the experiments and solutions, the CD values recorded at 222 nm were normalized by the respective value measured at 20 °C and plotted versus temperature. Melting temperatures were determined from the maximum of the first derivative calculated with the Spectra Analysis Software (Jasco). Experiments were conducted in at least triplicate.

Heparin Binding Assay. The heparin binding affinity of WT and mutant APP E2 was qualitatively determined by salt gradient elution from a 1.2 mL column packed with HiTrap Heparin Sepharose HP (GE Healthcare) connected to an Äkta

DOI: 10.1021/acs.biochem.5b00111
Biochemistry 2015, 54, 2490–2499

Micro chromatography system (GE Healthcare). After injection of 50 μg of protein, the column-bound sample was eluted with a linear 150 to 1000 mM NaCl gradient. Prior to Zn^{2+}- and Cu^{2+}-supplemented experiments, metals were added at a concentration of 50 μM to both the sample and the running buffer. Metal-free experiments were always performed in 5 mM Tris (pH 8.0). For measurements with zinc and copper, 20 mM Hepes (pH 8.0) and 50 mM Tris (pH 8.0), respectively, were used. Conductivities at the A_{280} peak maximum were measured in triplicate and converted to salt concentrations by standard curves. For statistical analysis, a two-tailed, unpaired t test was performed using Microsoft Excel. Significance was considered at 0.01, 0.05, and 0.1 levels.

Surface Plasmon Resonance Analysis. The sorLA fragment comprising the extracellular part was generated and immobilized onto CM5 (BIAcore) biosensor chips as previously described.[30] Approximately 70 fmol of sorLA/mm^2 was immobilized. The samples of E2-WT, E2-H313A, and E2-H382A were prepared in two different running buffers to test for the influence on the buffer system, either 10 mM Hepes (pH 7.4) or 50 mM Tris (pH 7.3) including 150 mM NaCl and 1.5 mM $CaCl_2$. The proteins were tested at a series of 5, 25, 50, 100, 200, and 500 nM concentrations, and binding kinetics were estimated using the *BIAevaluation* software with the approximation of a 1:1 Langmuir binding model. Regeneration of the chip surface was performed by alternating pulses of 10 mM glycine hydrochloride (pH 4.0), 20 mM EDTA, 500 mM NaCl, 0.005% Tween 20, and 0.001% SDS. All measurements were conducted on a BIAcore 3000 instrument (BIAcore, Uppsala, Sweden).

Analyses of the influence of copper and zinc ions were conducted in a similar manner, except the concentration of $CaCl_2$ was decreased to 0.5 mM and either 10 μM $CuCl_2$ or 10 μM $ZnCl_2$ was included in running and sample buffers.

RESULTS

Generation and Purification of APP E2 Mutants. Point mutations in APP E2 expression constructs of M1 site residues H313, H382, H432, and H436 to alanine were obtained by site-directed mutagenesis polymerase chain reaction of the WT APP E2 construct. The H432+436A double mutant was derived from the H432A mutant. Expression and purification protocols for mutant APP E2 were adopted from those used for the WT protein. During the purification, variations in affinity for the heparin column resin were observed for the mutants, which were further analyzed in detail. Final yields did not differ between WT and mutant proteins, and the native folding of the mutants was confirmed by CD spectroscopy in comparison to that of the WT (Figure 1 of the Supporting Information).

Analysis of Zinc and Copper Binding Affinities. From the analysis of the zinc- and copper-bound crystal structures of APP E2[10] and Figure 1, we expected that copper binding should be impaired by any single mutation, because all M1 site residues are involved in binding. For zinc binding, histidine 313 should be dispensable whereas the removal of any other histidine should cause a zinc binding defect.

To analyze changes in the binding affinities of zinc and copper caused by the introduced mutations, we measured their affinities for copper and zinc by ITC. All titrations of Cu^{2+} into APP E2 mutants result in similar integrated heats (Figure 2A). Signals show only slight variations around 0 μJ indicating the absence of endo- and exothermic events and thus the expected loss of copper binding.

Titrations of Zn^{2+} to the APP E2 mutants showed, interestingly, more varying effects. As expected, the H313A mutant exhibited strong exothermic zinc binding, nearly similar to that of the WT protein (Figure 2B). A fit with a multisite model resulted in a dissociation constant (K_{D1}) of 2.6 ± 1.1 μM for the first strong binding event with a stoichiometry n_1 of 0.74 ± 0.04. Both the value for the affinity and the stoichiometry are within error identical to those of WT APP E2 (Table 1). The determined binding enthalpy ΔH_1 of −18.8 ± 3.1 kJ/mol was also comparable to that of WT APP E2.

Table 1. Thermodynamic Parameters of Binding of Zinc to H313A APP E2

	H313A APP E2	WT APP E2[a]
K_{D1} (μM)	2.6 ± 1.9	3.9 ± 1.5
ΔH_1 (kJ/mol)	−18.8 ± 5.3	−16.6 ± 0.6
n_1	0.7 ± 0.1	0.7 ± 0.2

[a]Taken from ref 10 for comparison.

Titration of Zn^{2+} to the H382A mutant of the APP E2 domain reveals a complete loss of tight zinc binding, as expected. The exothermic signals observed for WT APP E2 were missing; only weak endothermic signals of approximately 10 μJ were produced instead (Figure 2C), probably caused by the unspecific binding sites for Zn^{2+}.

Surprisingly, the H432A mutation does not completely deplete zinc binding, which is evident from the occurrence of small exothermic signals during titrations (Figure 2D). However, no significant fit to the data and hence no thermodynamic parameters could be obtained. Weaker zinc binding is indicated for the H436A and H432+436A mutants (Figure 2E,F). Although heat signals are endothermic throughout the whole titration, their initial reduction suggests that weak exothermic events occur but are covered by stronger endothermic signals. Hence, zinc binding is weak but still present for the H432A, H436A, and H432+436A mutants, especially when compared to that of the H382A mutant.

Metal Binding-Induced Stabilization of APP E2 Folding. We previously observed that binding of copper and zinc ions to the M1 site of APP E2 results in stabilization, which can be measured by an increased protein melting temperature.[10] In addition to characterizing the thermodynamic properties of our mutants by ITC, we thus also investigated their thermal stabilization by CD-based melting curves. For easy comparison, the respective WT data are reproduced in Figure 3A.

Consistent with our initial assumption and our results from ITC, copper does not show an effect on the thermal stability of APP E2 for any M1 site mutant, further underscoring that all four histidines of the M1 site are required for the binding of Cu^{2+} (Figure 3, gray curves).

When Zn^{2+} is added to the H313A mutated APP E2 domain, it becomes thermally stabilized, which is apparent in a shift of the melting curve (Figure 3B, black) and an increase in melting temperature from 57.7 ± 0.3 to 65.0 ± 1.0 °C, which is comparable to that of APP E2 WT (Table 2). Interestingly, similar changes of the melting curves were observed for the H432A and H436A mutants (Figure 3C,D, black), which exhibit increases in T_M from 57.7 ± 0.3 to 63.2 ± 0.4 °C and from 58.3 ± 0.3 to 62 ± 0.0 °C, respectively (Table 2). Consistent with the ITC data, the H382A mutant showed no stabilization effect upon the addition of zinc (Figure 3E). A

DOI: 10.1021/acs.biochem.5b00111
Biochemistry 2015, 54, 2490−2499

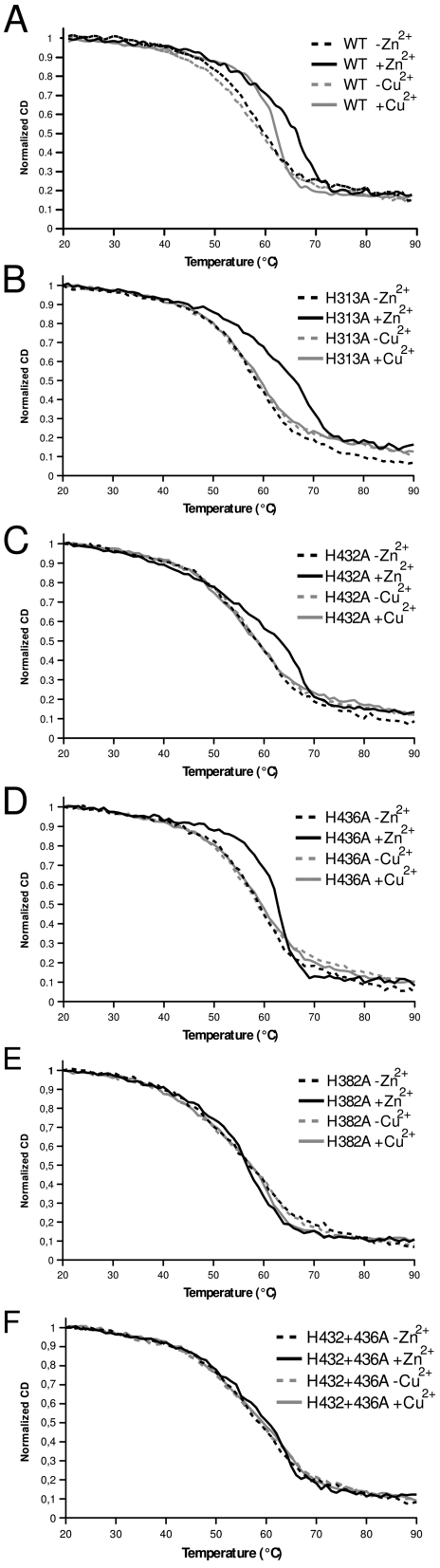

Figure 3. CD melting curves of WT and mutant APP E2: (A) WT, (B) H313A, (C) H432A, (D) H436A, (E) H382A, and (F) H432+436A. Curves represent the average of at least three independent experiments. Control measurements without metals are drawn as dashed lines. The WT data are taken from ref 10 for comparison.

small effect on thermostability was still observed for the H432+436A double mutant, evidenced by a slight increase in the melting temperature of 1.7 °C (Figure 3F, black, and Table 2).

Taken together, all mutants did not show any measurable copper binding. The removal of His313 does not change the Zn^{2+} binding properties of APP E2. In contrast, the H382A mutation causes a complete loss of zinc binding. Mutants H432A and H436A and the double mutant show a reduced level of zinc binding. In addition, the mutations H436A and to a lesser degree also H432A and the H432+436A double mutant show an increased cooperativity (indicated by a steeper decay of the α-helical signal in the CD-based melting curves) during thermal denaturation (Figure 3B,C,E), similar to that observed upon binding of copper to the wild-type protein.[10]

Heparin Binding. On the basis of conformational changes present in zinc- and copper-bound X-ray structures of APP E2, it has been suggested that binding of metal ions to the M1 site may regulate interactions of the APP E2 domain with interaction partners,[10] and a dependency of heparin binding on Zn^{2+} concentration has been described.[29] Next, we therefore characterized the M1 site mutants for copper- and zinc-induced changes in heparin binding to examine a regulatory role of binding of metal to the M1 site. To study this, WT and mutant APP E2 were bound to a heparin column and eluted by a linear salt gradient. According to the manufacturer, the heparin resin was purified from porcine intestine mucosa (native source) and is composed of varyingly substituted D-glucoronic acid, L-iduronic acid, and D-glucoseamine moieties. All three sugar variants have been shown to specifically bind the E2 domain of APLP1,[42,43] a close APP homologue. Hence, we assumed a binding environment close to the physiological situation. Differences in the salt concentration required for release of the respective protein from the heparin resin correspond hereby to altered binding strengths.

The WT APP E2 domain elutes at a NaCl concentration of 489 mM from the heparin column (Figure 4). Compared to that, the H313A and H382A mutations cause a significant ($p < 0.01$) decrease in heparin affinity as these mutants elute earlier in the gradient at 440 and 458 mM NaCl, respectively. The H432A-mutated APP E2 domain elutes at a salt concentration basically identical to that of the WT protein. A slight decrease in heparin affinity can be observed upon comparison of the H436A and the H432+436A mutants to the WT APP E2 domain. They both elute at salt concentrations slightly but significantly ($p < 0.01$) below that of the WT (482 and 484 mM, respectively).

The influence of Zn^{2+} and Cu^{2+} on heparin affinity was tested by the addition of 50 μM $ZnCl_2$ or $CuCl_2$. The addition of Zn^{2+} to WT E2 caused an increased salt concentration of 524 mM NaCl needed for elution from the heparin column indicating stronger binding (Figure 4) as previously observed.[29] Copper-(II) ions lead to an even stronger affinity as evidenced by a shifted elution in the gradient to 550 mM NaCl. Cu^{2+} ions were not added to the mutants as they were already shown not to bind Cu^{2+} (i.e., Figure 3). When Zn^{2+} was added to the H313A mutant, the affinity for heparin increased significantly ($p < 0.01$) as evidenced by the elution of the protein at 478 mM NaCl. The protein elutes, however, still at lower NaCl concentrations compared to those in the same experiments with WT protein, suggesting that histidine 313 is directly involved in mediating the Zn^{2+}-dependent effect on heparin binding. Heparin binding of the H382A mutant, which does not

DOI: 10.1021/acs.biochem.5b00111
Biochemistry 2015, 54, 2490−2499

Table 2. Melting Temperatures (T_M) Determined by CD Melting Curve Experiments and Occurrence of Cooperativity As Observed by an Increased $\Delta CD/\Delta T$ at the Melting Temperature

	T_M (°C)			T_M (°C)		
	without Zn^{2+}	with Zn^{2+}	cooperativity	without Cu^{2+}	with Cu^{2+}	cooperativity
WT[a]	57.8 ± 0.3	64.2 ± 0.3	−	57.3 ± 0.3	61.0 ± 0.0	+
H313A	57.7 ± 0.3	65.0 ± 1.0	−	57.0 ± 0.0	57.3 ± 0.3	−
H432A	57.7 ± 0.3	63.2 ± 0.4	(+)	56.7 ± 0.3	57.0 ± 0.6	−
H436A	58.3 ± 0.3	62.0 ± 0.0	+	57.3 ± 0.3	58.7 ± 0.3	−
H382A	56.0 ± 0.0	56.5 ± 0.7	−	57.0 ± 0.0	56.7 ± 0.3	−
H432+436A	57.3 ± 0.3	59.0 ± 0.0	−[b]	58.0 ± 0.6	58.3 ± 0.6	−

[a]Taken from ref 10 for comparison. [b]Slight cooperativity visible upon closer examination.

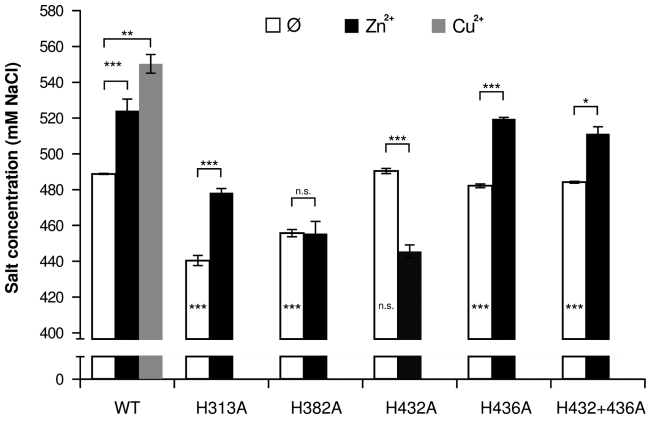

Figure 4. Salt concentrations determined at elution peak maxima from the heparin column. Metal-free (white) as well as Zn^{2+}- and Cu^{2+}-supplemented (black and gray, respectively) experiments are shown. Bars represent the mean of at least three independent experiments with the indicated standard deviation. Asterisks in the bars represent significance levels for differences to the respective measurement with WT protein. The significance for pairwise comparisons is indicated above the bars. Three asterisks, two asterisks, and one asterisk indicate $p < 0.01$, 0.05, and 0.1, respectively.

bind zinc at the M1 site, is not significantly affected by the addition of Zn^{2+}.

Mutant H436A and the double mutant both show significantly ($p < 0.01$ and 0.1, respectively) increased heparin affinity upon addition of zinc. Their zinc-induced affinity for heparin is overall similar as they elute at 519 and 522 mM salt, respectively. Surprisingly and in contrast to the other mutants, the H432A mutant exhibits a decreased heparin affinity in the presence of Zn^{2+}, which is visible by an elution at 445 mM NaCl. These data suggest that Zn^{2+} induces an effect in APP E2 H432A different from that observed with the other mutants.

Surface Plasmon Resonance Analysis of the Binding of APP E2 to sorLA. We next investigated the interaction of sorLA with WT APP E2 and the H313A and H382A mutants as well as its dependence on Zn^{2+} and Cu^{2+} ions. The luminal part of sorLA was purified and immobilized onto a biacore sensor chip as previously described.[30] We tested binding of APP E2 WT, H313A, and H382A at 5−500 nM in both a Hepes-buffered assay and a Tris-buffered assay (Figure 5). Both assays show an indistinguishable interaction between sorLA and any of the three tested APP E2 proteins. The affinities were estimated to represent K_D values at 6, 7, and 5 nM and 17, 19, and 17 nM for WT, H313A, and H382A proteins, respectively, when measured in either Tris- or Hepes-buffered samples. From this experiment, we conclude that these mutations do not per se alter the ability of APP E2 to bind sorLA.

We next supplemented the running buffer with either 10 μM Cu^{2+} (in Tris) or 10 μM Zn^{2+} (in Hepes) and repeated the SPR binding analysis. No significant difference was observed for mutant or metal ion (data not shown). We observed a certain trend only toward an increased affinity between sorLA and the H382A mutant in the presence of Zn^{2+}, which was indeed very surprising as this mutant was shown not to bind Zn^{2+}. We currently do, however, not know whether copper and zinc ions possibly bind to sorLA, nor do we know in which way the binding of Zn^{2+} ions at sites other than M1 possibly affect the interaction between sorLA and APP E2. Thus, we are not able to dissect whether any observed changes in the presence of Zn^{2+} and Cu^{2+} are actually attributed to interactions between sorLA and APP E2 M1. Accordingly, we did not continue those studies and conclude that neither the H313A mutation nor the H382A mutation leads to any change in binding between sorLA and APP E2 in the current experimental setup.

DISCUSSION

The M1 metal binding site in the APP E2 domain has been discovered just recently.[10] Because the homeostasis of copper and zinc is thought to play a significant role in AD, zinc and/or copper binding deficient M1 site mutants would provide a powerful tool for investigating the influence of metal binding to APP function and AD. This work provides an extensive characterization of M1 site mutants that are deficient in copper binding and exhibit either nonaltered, weakened, or abolished zinc binding to M1, while retaining a native protein conformation.

When we tested for copper binding, all examined mutants did not show any significant heat associated with binding events or thermal stabilization of the protein fold in CD melting curves, which shows that all mutants no longer bind Cu^{2+}. That is in agreement with the requirement of all four M1 site histidines (i.e., H313, H382, H432, and H436) reported for copper coordination by the M1 site.[10] Interestingly, zinc binding experiments revealed more varying effects. For the H313A mutant, a zinc binding affinity identical to that of the WT APP E2 domain could be determined, confirming the presence of a tridentate coordination by histidines 382, 432, and 436 as observed in the crystal structure of APP E2 bound to zinc (ref 10 and Figure 1A). Moreover, also the zinc-induced increase in thermal stability is comparable to that of WT APP E2, indicating that histidine 313 does not contribute to the stabilization of the protein fold upon zinc binding. Interestingly, the removal of histidines 432 or 436 did not lead to a complete loss of zinc binding, indicating a compensatory mechanism. Indeed, the cooperative denaturation observed in CD melting curves of the H432 and H436 mutants resembles the behavior of WT APP E2 bound to copper.[10] One structural explanation

DOI: 10.1021/acs.biochem.5b00111
Biochemistry 2015, 54, 2490−2499

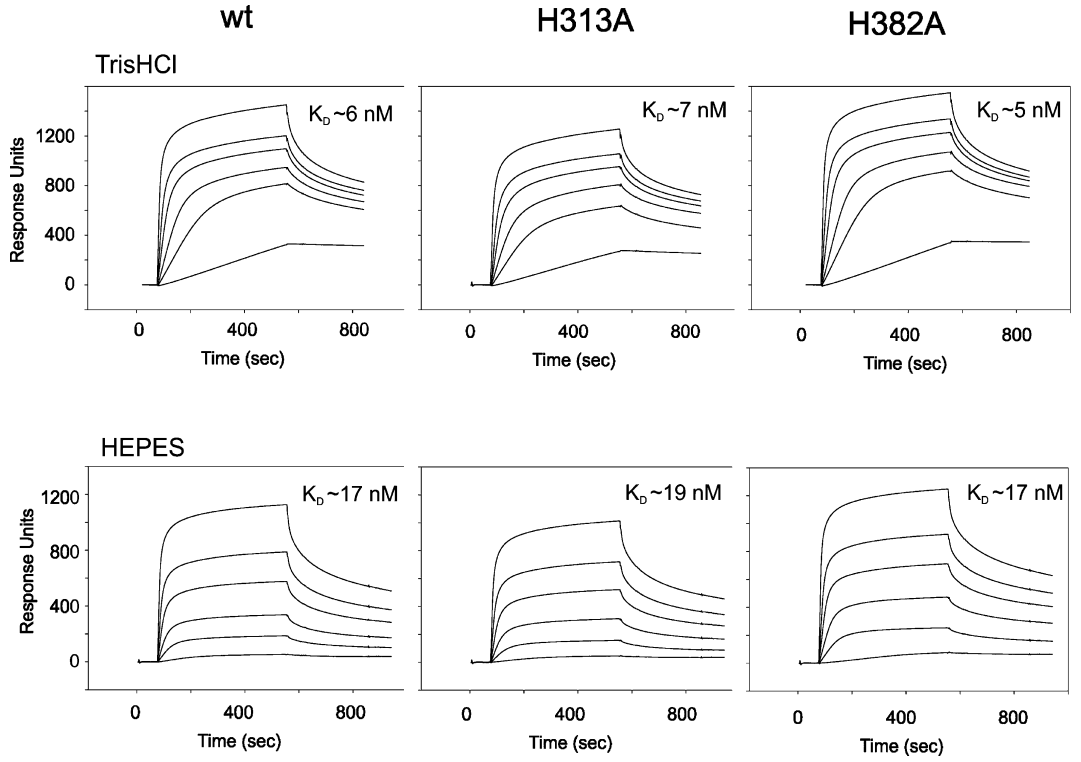

Figure 5. Surface plasmon resonance analysis of APP E2 variants binding to immobilized sorLA. E2 WT, H313A, and H382A were analyzed at increasing concentrations of 5, 25, 50, 100, 200, and 500 nM in either Tris-buffered samples (top) or Hepes-buffered samples (bottom). The affinities (dissociation constants, K_D) for the interaction were estimated using BIAevaluation.

might be that histidine 313 swings into the M1 site and thereby functionally compensates for missing histidine 432 or 436, explaining the binding behavior, the observed thermal stabilization of the mutants by Zn^{2+}, and the increased cooperativity. A similar compensation is also indicated for APLP1, in which all four M1 site histidines are conserved,[10] as the removal of H430 (corresponding to H436 in APP) does not alter its sensitivity for zinc.[22] Although the experimental data available support such a mechanism, structural confirmation of the swing-in by H313 is not available.

In contrast, the removal of H382 caused a complete loss of zinc binding in ITC and CD spectroscopy. To understand why such a compensatory mechanism for binding of Zn^{2+} to M1 is possible for H432 and H436 but not for H382, we examined the local protein environment. We identified a π-stacking interaction between histidine 382 and phenylalanine 316 in all known structures of E2 domains of APP or APP-like proteins (Figure 2A–G of the Supporting Information). It may anchor the α-helix containing H313 to position it in the proximity of the M1 site, and thus, it seems essential for the proposed swing-in of H313. Furthermore, the presence of an aromatic residue according to F316 in human APP_{695} is highly conserved (Figure 2H of the Supporting Information).

In previous studies, an increased affinity of heparin for its binding region in APP E2 has been reported to be caused by zinc, however, for a putative zinc binding site apart from the E2 domain.[29] Using the wild-type APP E2 domain, we could observe a similar Zn^{2+}-induced enhancement of heparin affinity. Moreover, Cu^{2+} could induce an even stronger effect. The mutant H313A, which binds Zn^{2+} like the WT protein at M1, shows the expected increase in heparin binding affinity upon incubation with zinc. The overall reduction in binding strength indicates, however, that histidine 313 itself might be important for the interaction between APP E2 and heparin. The H382A mutant, which completely abolishes Zn binding, also shows no effect of zinc ions on the binding of heparin. This clearly demonstrates that binding of metal to M1 affects the heparin affinity of the E2 domain.

H432A, H436A, and double mutant H432+436A show, as for the stabilization discussed above, differing effects on heparin binding. Whereas H436A and H432+436A show an increased level of heparin binding upon incubation with Zn^{2+} as expected from their ability to bind the metal ions, the H432A mutant shows a reduced heparin affinity upon incubation with Zn^{2+}. This is most likely caused by a structural rearrangement of the H432A mutant to gain a higher affinity for the ion while losing the integrity of the heparin binding site.

Previous studies biochemically mapped the heparin binding site for the E2 domain of human APLP1 (hAPLP1) as well as for APL-1 of *Caenorhabditis elegans* (cAPL-1) by mutational analysis.[42,44,45] Because the M1 mutations overlap with some of the previously analyzed residues, we could examine their contribution to heparin binding to the here studied human APP. The reduced affinity observed for the H313A and H436A mutants indicates a direct involvement of those side chains in binding of heparin to APP E2, which is in agreement with previous results for hAPLP1 and cAPL-1 (Table 1 of the Supporting Information). The decreased heparin affinity induced by the H382A mutation is most likely caused by the discussed loss of the π-stacking interaction with F316 concomitant with the delocalization of histidine 313, which also would explain previous observations.

Because of the nature of the column-based assay, nonspecific electrostatic interactions with the high charge density of the heparin resin likely contribute to the described affinities. However, because removal of uncharged side chains causes

DOI: 10.1021/acs.biochem.5b00111
Biochemistry 2015, 54, 2490–2499

large effects although the protein remains properly folded (e.g., H313A), information about specific interactions can be derived.

Thus, mutant H313A, which affects only the binding of Cu^{2+} but not the binding of Zn^{2+} to the M1 site, and mutant H382A, which completely abolishes binding of either metal ion to M1, should prove to be most useful for subsequent functional studies of M1. These mutants give together with the WT protein clear-cut results with respect to the binding of heparin and were subsequently used to analyze the impact of M1 on the interaction between APP E2 and sorLA. The other mutants (H432A, H436A, and H432+436A) are less suited for such studies because of additional compensatory or unspecific effects.

The Zn^{2+}- and Cu^{2+}-dependent modulation of binding of heparin to the APP E2 domain described in this study gives some insight into the interplay between zinc and copper ions present in the brain and the function of APP. The highest levels of neuronal APP expression are found in the early stages of postnatal brain development, and its function to bind to the extracellular matrix is thought to play a significant role in this process (reviewed, e.g., in ref 32). Binding of zinc and copper to M1 positively regulates the affinity of APP E2 for heparin and hence may influence the formation of synapses, neurite outgrowth, and dendritic spine formation and maintenance. Interestingly, during rat brain development, zinc levels significantly increase in regions involved in learning, long-term memory, and movement.[46] Because zinc and copper induce effects to different extents, they also may act differentially. Indeed, copper levels also increase during early life span, however, mostly in regions that are not characterized by elevated zinc concentrations,[46] suggesting discrete roles for both ions. In AD brains, dysregulated zinc and copper levels have been reported; however, these studies are divergent about increased or decreased levels.[47] Pathologically altered zinc and copper concentrations might not only contribute to Aβ oligomerization and plaque formation but also affect normal APP function as a cell adhesion protein for maintaining synapses and dendritic spines.

The subcellular localization of APP influences its adherence to a non-amyloidogenic pathway or Aβ production, and copper has been shown to increase the level of exocytosis of APP.[21,48] Therefore, we examined the influence of mutations H313A and H382A as well as of zinc and copper binding on the interaction of APP E2 with its sorting receptor sorLA that is also known to regulate the intracellular trafficking of APP.[30,36,49]

We did not observe any effect of the mutations within the M1 site on binding of APP E2 to sorLA. This shows that both residues, H313 and H382, are not directly involved in the interaction between sorLA and APP E2. Surprisingly and in parallel, we also did not find any indication that the interaction between sorLA and APP is influenced by variations in zinc and copper concentrations. Whereas at first unexpected, this finding agrees well with the function of sorLA as a binding partner of APP within the Golgi compartments. The concentration of copper and zinc does probably not change as a function of synaptic activity here. It will be interesting to see if other interactors of APP E2, such as the low-density lipoprotein receptor-related protein 1 (LRP1)[50] or F-Spondin,[15] that are reported to interact with APP at the cell surface show a metal dependence in their interaction strength, potentially similar to that observed for the extracellular ligand heparin. This would fit a model in which LRP1 is known to bind most of its ligands in a heparin-dependent manner, suggesting that the APP binding epitopes are shared among heparin and LRP1.

■ ASSOCIATED CONTENT

Supporting Information

CD spectra recorded for the mutants, sequence alignment and structural comparison of APP and APP-like proteins, and a summary of mutations affecting binding of heparin to APP E2. This material is available free of charge via the Internet at http://pubs.acs.org.

■ AUTHOR INFORMATION

Corresponding Author

*E-mail: than@fli-leibniz.de. Telephone: (+49) 3641-656170.

Present Address

§C.D.: Department of Molecular Biology, Max-Planck-Institute for Biophysical Chemistry, Am Fassberg 11, 37077 Göttingen, Germany.

Funding

Studies in the Andersen laboratory are funded by the Novo Nordic Foundation (Grant R179-A15311) and the Lundbeck Foundation (Grant R93-A8578), and the Leibniz Institute for Age Research (FLI) is funded by the Federal Government of Germany and the State of Thuringia.

Notes

The authors declare no competing financial interest.

■ ABBREVIATIONS

Aβ, amyloid β; AcD, acidic domain; AD, Alzheimer's disease; AICD, APP intracellular domain; APP, amyloid precursor protein; APLP/APL, APP-like protein; CAPPD, central APP domain; CD, circular dichroism; GWAS, genomewide association studies; ITC, isothermal titration calorimetry; JMR, juxtamembrane region; KPI, Kunitz protease inhibitor; LOAD, late onset Alzheimer's disease; WT, wild-type.

■ REFERENCES

(1) Jellinger, K. A. (2006) Clinicopathological analysis of dementia disorders in the elderly: An update. *J. Alzheimer's Dis. 9*, 61−70.

(2) Thies, W., and Bleiler, L. (2013) 2013 Alzheimer's Disease Facts and Figures. *Alzheimers Dement. 9*, 208−245.

(3) Thinakaran, G., and Koo, E. H. (2008) Amyloid precursor protein trafficking, processing, and function. *J. Biol. Chem. 283*, 29615−29619.

(4) Hardy, J., and Selkoe, D. J. (2002) The amyloid hypothesis of Alzheimer's disease: Progress and problems on the road to therapeutics. *Science 297*, 353−356.

(5) Blennow, K., de Leon, M. J., and Zetterberg, H. (2006) Alzheimer's disease. *Lancet 368*, 387−403.

(6) Golde, T. E., Schneider, L. S., and Koo, E. H. (2011) Anti-Aβ therapeutics in Alzheimer's disease: The need for a paradigm shift. *Neuron 69*, 203−213.

(7) Lichtenthaler, S. F., Haass, C., and Steiner, H. (2011) Regulated intramembrane proteolysis: Lessons from amyloid precursor protein processing. *J. Neurochem. 117*, 779−796.

(8) Milward, E. A., Papadopoulos, R., Fuller, S. J., Moir, R. D., Small, D., Beyreuther, K., and Masters, C. L. (1992) The amyloid protein precursor of Alzheimer's disease is a mediator of the effects of nerve growth factor on neurite outgrowth. *Neuron 9*, 129−137.

(9) Kepp, K. P. (2012) Bioinorganic chemistry of Alzheimer's disease. *Chem. Rev. 112*, 5193−5239.

(10) Dahms, S. O., Konnig, I., Roeser, D., Guhrs, K. H., Mayer, M. C., Kaden, D., Multhaup, G., and Than, M. E. (2012) Metal binding

DOI: 10.1021/acs.biochem.5b00111
Biochemistry 2015, 54, 2490−2499

dictates conformation and function of the amyloid precursor protein (APP) E2 domain. *J. Mol. Biol. 416*, 438−452.
(11) von Rotz, R. C., Kohli, B. M., Bosset, J., Meier, M., Suzuki, T., Nitsch, R. M., and Konietzko, U. (2004) The APP intracellular domain forms nuclear multiprotein complexes and regulates the transcription of its own precursor. *J. Cell Sci. 117*, 4435−4448.
(12) Muller, T., Concannon, C. G., Ward, M. W., Walsh, C. M., Tirniceriu, A. L., Tribl, F., Kogel, D., Prehn, J. H., and Egensperger, R. (2007) Modulation of gene expression and cytoskeletal dynamics by the amyloid precursor protein intracellular domain (AICD). *Mol. Biol. Cell 18*, 201−210.
(13) Breen, K. C., Bruce, M., and Anderton, B. H. (1991) β amyloid precursor protein mediates neuronal cell-cell and cell-surface adhesion. *J. Neurosci. Res. 28*, 90−100.
(14) Soba, P., Eggert, S., Wagner, K., Zentgraf, H., Siehl, K., Kreger, S., Lower, A., Langer, A., Merdes, G., Paro, R., Masters, C. L., Muller, U., Kins, S., and Beyreuther, K. (2005) Homo- and heterodimerization of APP family members promotes intercellular adhesion. *EMBO J. 24*, 3624−3634.
(15) Ho, A., and Sudhof, T. C. (2004) Binding of F-spondin to amyloid-β precursor protein: A candidate amyloid-β precursor protein ligand that modulates amyloid-β precursor protein cleavage. *Proc. Natl. Acad. Sci. U.S.A. 101*, 2548−2553.
(16) Koo, E. H., Sisodia, S. S., Archer, D. R., Martin, L. J., Weidemann, A., Beyreuther, K., Fischer, P., Masters, C. L., and Price, D. L. (1990) Precursor of amyloid protein in Alzheimer disease undergoes fast anterograde axonal transport. *Proc. Natl. Acad. Sci. U.S.A. 87*, 1561−1565.
(17) Parvathy, S., Hussain, I., Karran, E. H., Turner, A. J., and Hooper, N. M. (1999) Cleavage of Alzheimer's amyloid precursor protein by α-secretase occurs at the surface of neuronal cells. *Biochemistry 38*, 9728−9734.
(18) Koo, E. H., and Squazzo, S. L. (1994) Evidence that production and release of amyloid β-protein involves the endocytic pathway. *J. Biol. Chem. 269*, 17386−17389.
(19) Dries, D. R., and Yu, G. (2008) Assembly, maturation, and trafficking of the γ-secretase complex in Alzheimer's disease. *Curr. Alzheimer Res. 5*, 132−146.
(20) Andersen, O. M., Reiche, J., Schmidt, V., Gotthardt, M., Spoelgen, R., Behlke, J., von Arnim, C. A., Breiderhoff, T., Jansen, P., Wu, X., Bales, K. R., Cappai, R., Masters, C. L., Gliemann, J., Mufson, E. J., Hyman, B. T., Paul, S. M., Nykjaer, A., and Willnow, T. E. (2005) Neuronal sorting protein-related receptor sorLA/LR11 regulates processing of the amyloid precursor protein. *Proc. Natl. Acad. Sci. U.S.A. 102*, 13461−13466.
(21) Acevedo, K. M., Hung, Y. H., Dalziel, A. H., Li, Q. X., Laughton, K., Wikhe, K., Rembach, A., Roberts, B., Masters, C. L., Bush, A. I., and Camakaris, J. (2011) Copper promotes the trafficking of the amyloid precursor protein. *J. Biol. Chem. 286*, 8252−8262.
(22) Mayer, M. C., Kaden, D., Schauenburg, L., Hancock, M. A., Voigt, P., Roeser, D., Barucker, C., Than, M. E., Schaefer, M., and Multhaup, G. (2014) Novel zinc-binding site in the E2 domain regulates amyloid precursor-like protein 1 (APLP1) oligomerization. *J. Biol. Chem. 289*, 19019−19030.
(23) Barnham, K. J., and Bush, A. I. (2008) Metals in Alzheimer's and Parkinson's diseases. *Curr. Opin. Chem. Biol. 12*, 222−228.
(24) Budimir, A. (2011) Metal ions, Alzheimer's disease and chelation therapy. *Acta Pharm. (Zagreb, Croatia) 61*, 1−14.
(25) Bayer, T. A., Cappai, R., Masters, C. L., Beyreuther, K., and Multhaup, G. (1999) It all sticks together: The APP-related family of proteins and Alzheimer's disease. *Mol. Psychiatry 4*, 524−528.
(26) Coburger, I., Dahms, S. O., Roeser, D., Guhrs, K. H., Hortschansky, P., and Than, M. E. (2013) Analysis of the overall structure of the multi-domain amyloid precursor protein (APP). *PLoS One 8*, e81926.
(27) Coburger, I., Hoefgen, S., and Than, M. E. (2014) The structural biology of the amyloid precursor protein APP: A complex puzzle reveals its multi-domain architecture. *Biol. Chem. 395*, 485−498.
(28) Zheng, H., and Koo, E. H. (2006) The amyloid precursor protein: Beyond amyloid. *Mol. Neurodegener. 1*, 5.
(29) Multhaup, G., Mechler, H., and Masters, C. L. (1995) Characterization of the high affinity heparin binding site of the Alzheimer's disease β A4 amyloid precursor protein (APP) and its enhancement by zinc(II). *J. Mol. Recognit. 8*, 247−257.
(30) Andersen, O. M., Schmidt, V., Spoelgen, R., Gliemann, J., Behlke, J., Galatis, D., McKinstry, W. J., Parker, M. W., Masters, C. L., Hyman, B. T., Cappai, R., and Willnow, T. E. (2006) Molecular dissection of the interaction between amyloid precursor protein and its neuronal trafficking receptor SorLA/LR11. *Biochemistry 45*, 2618−2628.
(31) Schubert, D., LaCorbiere, M., Saitoh, T., and Cole, G. (1989) Characterization of an amyloid β precursor protein that binds heparin and contains tyrosine sulfate. *Proc. Natl. Acad. Sci. U.S.A. 86*, 2066−2069.
(32) Hoe, H. S., Lee, H. K., and Pak, D. T. (2012) The upside of APP at synapses. *CNS Neurosci. Ther. 18*, 47−56.
(33) Rogaeva, E., Meng, Y., Lee, J. H., Gu, Y., Kawarai, T., Zou, F., Katayama, T., Baldwin, C. T., Cheng, R., Hasegawa, H., Chen, F., Shibata, N., Lunetta, K. L., Pardossi-Piquard, R., Bohm, C., Wakutani, Y., Cupples, L. A., Cuenco, K. T., Green, R. C., Pinessi, L., Rainero, I., Sorbi, S., Bruni, A., Duara, R., Friedland, R. P., Inzelberg, R., Hampe, W., Bujo, H., Song, Y. Q., Andersen, O. M., Willnow, T. E., Graff-Radford, N., Petersen, R. C., Dickson, D., Der, S. D., Fraser, P. E., Schmitt-Ulms, G., Younkin, S., Mayeux, R., Farrer, L. A., and St George-Hyslop, P. (2007) The neuronal sortilin-related receptor SORL1 is genetically associated with Alzheimer disease. *Nat. Genet. 39*, 168−177.
(34) Lambert, J. C., Ibrahim-Verbaas, C. A., Harold, D., Naj, A. C., Sims, R., Bellenguez, C., DeStafano, A. L., Bis, J. C., Beecham, G. W., Grenier-Boley, B., Russo, G., Thorton-Wells, T. A., Jones, N., Smith, A. V., Chouraki, V., Thomas, C., Ikram, M. A., Zelenika, D., Vardarajan, B. N., Kamatani, Y., Lin, C. F., Gerrish, A., Schmidt, H., Kunkle, B., Dunstan, M. L., Ruiz, A., Bihoreau, M. T., Choi, S. H., Reitz, C., Pasquier, F., Cruchaga, C., Craig, D., Amin, N., Berr, C., Lopez, O. L., De Jager, P. L., Deramecourt, V., Johnston, J. A., Evans, D., Lovestone, S., Letenneur, L., Moron, F. J., Rubinsztein, D. C., Eiriksdottir, G., Sleegers, K., Goate, A. M., Fievet, N., Huentelman, M. W., Gill, M., Brown, K., Kamboh, M. I., Keller, L., Barberger-Gateau, P., McGuiness, B., Larson, E. B., Green, R., Myers, A. J., Dufouil, C., Todd, S., Wallon, D., Love, S., Rogaeva, E., Gallacher, J., St George-Hyslop, P., Clarimon, J., Lleo, A., Bayer, A., Tsuang, D. W., Yu, L., Tsolaki, M., Bossu, P., Spalletta, G., Proitsi, P., Collinge, J., Sorbi, S., Sanchez-Garcia, F., Fox, N. C., Hardy, J., Deniz Naranjo, M. C., Bosco, P., Clarke, R., Brayne, C., Galimberti, D., Mancuso, M., Matthews, F., European Alzheimer's Disease, I., Genetic, Environmental Risk in Alzheimer's, D., Alzheimer's Disease Genetic, C., Cohorts for, H., Aging Research in Genomic, E., Moebus, S., Mecocci, P., Del Zompo, M., Maier, W., Hampel, H., Pilotto, A., Bullido, M., Panza, F., Caffarra, P., Nacmias, B., Gilbert, J. R., Mayhaus, M., Lannefelt, L., Hakonarson, H., Pichler, S., Carrasquillo, M. M., Ingelsson, M., Beekly, D., Alvarez, V., Zou, F., Valladares, O., Younkin, S. G., Coto, E., Hamilton-Nelson, K. L., Gu, W., Razquin, C., Pastor, P., Mateo, I., Owen, M. J., Faber, K. M., Jonsson, P. V., Combarros, O., O'Donovan, M. C., Cantwell, L. B., Soininen, H., Blacker, D., Mead, S., Mosley, T. H., Jr., Bennett, D. A., Harris, T. B., Fratiglioni, L., Holmes, C., de Bruijn, R. F., Passmore, P., Montine, T. J., Bettens, K., Rotter, J. I., Brice, A., Morgan, K., Foroud, T. M., Kukull, W. A., Hannequin, D., Powell, J. F., Nalls, M. A., Ritchie, K., Lunetta, K. L., Kauwe, J. S., Boerwinkle, E., Riemenschneider, M., Boada, M., Hiltuenen, M., Martin, E. R., Schmidt, R., Rujescu, D., Wang, L. S., Dartigues, J. F., Mayeux, R., Tzourio, C., Hofman, A., Nothen, M. M., Graff, C., Psaty, B. M., Jones, L., Haines, J. L., Holmans, P. A., Lathrop, M., Pericak-Vance, M. A., Launer, L. J., Farrer, L. A., van Duijn, C. M., Van Broeckhoven, C., Moskvina, V., Seshadri, S., Williams, J., Schellenberg, G. D., and Amouyel, P. (2013) Meta-analysis of 74,046 individuals identifies 11 new susceptibility loci for Alzheimer's disease. *Nat. Genet. 45*, 1452−1458.

DOI: 10.1021/acs.biochem.5b00111
Biochemistry 2015, 54, 2490−2499

(35) Miyashita, A., Koike, A., Jun, G., Wang, L. S., Takahashi, S., Matsubara, E., Kawarabayashi, T., Shoji, M., Tomita, N., Arai, H., Asada, T., Harigaya, Y., Ikeda, M., Amari, M., Hanyu, H., Higuchi, S., Ikeuchi, T., Nishizawa, M., Suga, M., Kawase, Y., Akatsu, H., Kosaka, K., Yamamoto, T., Imagawa, M., Hamaguchi, T., Yamada, M., Morihara, T., Takeda, M., Takao, T., Nakata, K., Fujisawa, Y., Sasaki, K., Watanabe, K., Nakashima, K., Urakami, K., Ooya, T., Takahashi, M., Yuzuriha, T., Serikawa, K., Yoshimoto, S., Nakagawa, R., Kim, J. W., Ki, C. S., Won, H. H., Na, D. L., Seo, S. W., Mook-Jung, I., Alzheimer Disease Genetics, C., St George-Hyslop, P., Mayeux, R., Haines, J. L., Pericak-Vance, M. A., Yoshida, M., Nishida, N., Tokunaga, K., Yamamoto, K., Tsuji, S., Kanazawa, I., Ihara, Y., Schellenberg, G. D., Farrer, L. A., and Kuwano, R. (2013) SORL1 is genetically associated with late-onset Alzheimer's disease in Japanese, Koreans and Caucasians. *PLoS One 8*, e58618.

(36) Fjorback, A. W., Seaman, M., Gustafsen, C., Mehmedbasic, A., Gokool, S., Wu, C., Militz, D., Schmidt, V., Madsen, P., Nyengaard, J. R., Willnow, T. E., Christensen, E. I., Mobley, W. B., Nykjaer, A., and Andersen, O. M. (2012) Retromer binds the FANSHY sorting motif in SorLA to regulate amyloid precursor protein sorting and processing. *J. Neurosci. 32*, 1467−1480.

(37) Mehmedbasic, A., Christensen, S. K., Nilsson, J., Ruetschi, U., Gustafsen, C., Poulsen, A. S., Rasmussen, R. W., Fjorback, A. N., Larson, G., and Andersen, O. M. (2015) SorLA complement-type repeat domains protect the amyloid precursor protein against processing. *J. Biol. Chem. 290*, 3359−3376.

(38) Offe, K., Dodson, S. E., Shoemaker, J. T., Fritz, J. J., Gearing, M., Levey, A. I., and Lah, J. J. (2006) The lipoprotein receptor LR11 regulates amyloid β production and amyloid precursor protein traffic in endosomal compartments. *J. Neurosci. 26*, 1596−1603.

(39) Bhalla, A., Vetanovetz, C. P., Morel, E., Chamoun, Z., Di Paolo, G., and Small, S. A. (2012) The location and trafficking routes of the neuronal retromer and its role in amyloid precursor protein transport. *Neurobiol. Dis. 47*, 126−134.

(40) Willnow, T. E., and Andersen, O. M. (2013) Sorting receptor SORLA: A trafficking path to avoid Alzheimer disease. *J. Cell Sci. 126*, 2751−2760.

(41) Keil, C., Huber, R., Bode, W., and Than, M. E. (2004) Cloning, expression, crystallization and initial crystallographic analysis of the C-terminal domain of the amyloid precursor protein APP. *Acta Crystallogr. D60*, 1614−1617.

(42) Xue, Y., Lee, S., and Ha, Y. (2011) Crystal structure of amyloid precursor-like protein 1 and heparin complex suggests a dual role of heparin in E2 dimerization. *Proc. Natl. Acad. Sci. U.S.A. 108*, 16229−16234.

(43) Dahms, S. O., Mayer, M., Roeser, D., Multhaup, G., and Than, M. E. (2015) Interaction of the amyloid precursor protein-like protein 1 (APLP1) E2 domain with heparan sulfate involves two distinct binding modes. *Acta Crystallogr. D71*, 494−504.

(44) Xue, Y., Lee, S., Wang, Y., and Ha, Y. (2011) Crystal structure of the E2 domain of amyloid precursor protein-like protein 1 in complex with sucrose octasulfate. *J. Biol. Chem. 286*, 29748−29757.

(45) Hoopes, J. T., Liu, X., Xu, X., Demeler, B., Folta-Stogniew, E., Li, C., and Ha, Y. (2010) Structural characterization of the E2 domain of APL-1, a *Caenorhabditis elegans* homolog of human amyloid precursor protein, and its heparin binding site. *J. Biol. Chem. 285*, 2165−2173.

(46) Tarohda, T., Yamamoto, M., and Amamo, R. (2004) Regional distribution of manganese, iron, copper, and zinc in the rat brain during development. *Anal. Bioanal. Chem. 380*, 240−246.

(47) Szewczyk, B. (2013) Zinc homeostasis and neurodegenerative disorders. *Front. Aging Neurosci. 5*, 33.

(48) Acevedo, K. M., Opazo, C. M., Norrish, D., Challis, L. M., Li, Q. X., White, A. R., Bush, A. I., and Camakaris, J. (2014) Phosphorylation of amyloid precursor protein at threonine 668 is essential for its copper-responsive trafficking in SH-SY5Y neuroblastoma cells. *J. Biol. Chem. 289*, 11007−11019.

(49) Schmidt, V., Sporbert, A., Rohe, M., Reimer, T., Rehm, A., Andersen, O. M., and Willnow, T. E. (2007) SorLA/LR11 regulates processing of amyloid precursor protein via interaction with adaptors GGA and PACS-1. *J. Biol. Chem. 282*, 32956−32964.

(50) Waldron, E., Heilig, C., Schweitzer, A., Nadella, N., Jaeger, S., Martin, A. M., Weggen, S., Brix, K., and Pietrzik, C. U. (2008) LRP1 modulates APP trafficking along early compartments of the secretory pathway. *Neurobiol. Dis. 31*, 188−197.

DOI: 10.1021/acs.biochem.5b00111
Biochemistry 2015, 54, 2490−2499